Korean Chem. Eng. Res., 56(1), 139-142 (2018)
https://doi.org/10.9713/kcer.2017.56.1.139
PISSN 0304-128X, EISSN 2233-9558

Preparation of Si/C Anode with PVA Nanocomposite for Lithium-ion Battery Using Electrospinning Method

Sung Il Choi, Ye Min Lee, Hui Cheol Jeong, Eun-Jin Jung*, Mi Sun Lee*, Jinyoung Kim*, Yong Ha Kim and Yong Sun Won†

Department of Chemical Engineering, Pukyong National University, 365, Sinseon-ro, Nam-gu, Busan, 48547, Korea
**Metallic Materials Research Group, Research Institute of Industrial Science & Technology, 67, Cheongam-ro, Nam-gu, Pohang, Gyeongsangbuk-do, 37673, Korea*
(Received 5 September 2017; Received in revised form 8 October 2017; accepted 16 October 2017)

Abstract – Silicon (Si) is a promising anode material for next-generation lithium ion batteries (LIBs) because of its high capacity of 4,200 mAh/g ($Li_{4.4}Si$ phase). However, the large volume expansion of Si during lithiation leads to electrical failure of electrode and rapid capacity decrease. Generally, a binder is homogeneously mixed with active materials to maintain electrical contact, so that Si needs a particular binding system due to its large volume expansion. Polyvinyl alcohol (PVA) is known to form a hydrogen bond with partially hydrolyzed silicon oxide layer on Si nanoparticles. However, the decrease of its cohesiveness followed by the repeated volume change of Si still remains unsolved. To overcome this problem, we have introduced the electrospinning method to weave active materials in a stable nanofibrous PVA structure, where stresses from the large volume change of Si can be contained. We have confirmed that the capacity retention of Si-based LIBs using electrospun PVA matrix is higher compared to the conservative method (only dissolving in the slurry); the 25th cycle capacity retention ratio based on the 2nd cycle was 37% for the electrode with electrospun PVA matrix, compared to 27% and 8% for the electrodes with PVdF and PVA binders.

Key words: Lithium ion battery, Silicon, Polyvinyl alcohol (PVA), Electrospinning

1. Introduction

There is an increasing need for high-capacity lithium-ion batteries (LIBs) due to their applications to electrically powered vehicles and grid energy storage systems. In their most conventional structure, LIBs contain graphite anodes (e.g., mesocarbon microbeads, MCMB) [1-3]. Various metals such as Al, Sn, Bi and Si have been known to alloy with large amounts of Li [4,5]. Silicon (Si) has thus been presented as an alternative anode material because the theoretical specific capacity of Si (4,200 mAh/g) is an order of magnitude higher than that of conventional graphite anodes (372 mAh/g). But the large volume changes of Si during lithium insertion and desertion have prevented its commercial application [6,7]. Pulverization and the resulting electrical failure have been recognized as one of the major causes of poor cycle retention of Si-based anodes [8-12].

Recent researches have reported a size-dependent fracture of Si nanoparticles during lithiation; that is, there exists a critical particle diameter of ~150 nm, below which the particles neither crack nor fracture upon the first lithiation, and above which the particles initially form surface cracks and then fractur due to the lithiation-induced swelling [13-15]. Even when the Si particles did not crack during lithium insertion and desertion, a rapid capacity loss resulted from the poor electrical contact between the particles attributed to the deprecated mechanical properties (i.e., poor adhesion) of the binder during the great volume expansion of Si [16-19].

Polyvinyl alcohol (PVA) containing numerous hydroxyl groups could be a good choice as a binder for high capacity Si anodes since the hydroxyl groups form hydrogen bonds with both active materials and the current collector [20]. Thus, PVA could replace existing binders, but the decrease of cohesiveness still remains unsolved upon the charge-discharge cycle and the resulting large volume change of Si.

To overcome this problem, we introduced the electrospinning method to weave active materials into a nanofibrous PVA structure. Electrospun PVA nanofibers in the anode are expected to preserve the electrical contact between the Si particles by sustaining overall structure of active materials stably despite their large volume change. A schematic presents the underlying idea of this study in Fig. 1. Finally,

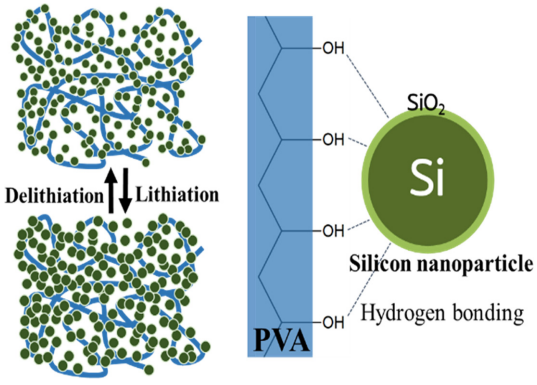

Fig. 1. Schematic of the proposed mechanism for the electrospun PVA anode.

† To whom correspondence should be addressed.
E-mail: yswon@pknu.ac.kr

we compared the capacity retention of Si/graphite-based LIBs with electrospun PVA electrode (hereafter, ESPVA-E) to those of the same Si/graphite-based LIBs with electrodes using PVdF (hereafter, PVdF-E) and PVA (hereafter, PVA-E) binders by electrochemical measurements. Si/graphite based LIBs were prepared (not prepared only with Si) because of the convenience in their preparation and performance measurements by the presence of conductive materials (graphite).

2. Material and Methods

2-1. Materials

Polyvinyl alcohol (PVA, average Mw = 30,000~50,000 and 130,000), Triton X-100, and dimethyl sulfoxide (DMSO) were purchased from Sigma-Aldrich and polyvinylidene fluoride (PVdF, average Mw = 600,000), N-Methyl-2-pyrrolidone (NMP), silicon nanopowder (99+%, 100 nm), mesocarbon microbeads graphite powder (MCMB, first discharge capacity: 345.2 mAh/g), and TIMCAL Super P conductive carbon black were purchased from MTI Korea. All the chemicals were used as received with no further purification.

2-2. Electrode preparation

The anode slurries were prepared by mixing PVA (Mw =30,000-50,000, 10 wt.%), Si nanopowder (25 wt%), MCMB (50 wt%), conductive carbon black (15 wt%) and DMSO (solvent) using a magnetic stirrer for 3 hrs to uniformity, and PVA and DMSO were replaced by PVdF and NMP at the same mass ratio for the PVdF-E electrode. The slurry was tape-casted onto a copper foil (10 mm thickness) current collector using the doctor-blade technique. The gap of the doctor blade was set to 150 mm. PVA-E and PVdF-E sheets were first dried on the hot plate at 70 °C for an hour and then dried in a vacuum oven at 140 °C overnight under vacuum condition.

2-3. Electrospinning process

PVA (Mw = 130,000, 10 wt%) was dissolved in distilled water by heating at 80 °C for 2 hrs with magnetic stirring. The solution was cooled to room temperature and then Triton X-100 was added as the surfactant. In a typical electrospinning process, PVA solution was transferred into a syringe and delivered to the tip of the syringe needle by the syringe pump at a constant feed rate (1.0 mL/h). A 20 kV positive voltage was applied to the PVA solution via a stainless steel syringe needle. The distance between the tip of the needle and the electrode sheet was about 15 cm. PVA solution was electrospun on the undried electrode sheet for an hour. ESPVA-E sheet was first dried on the hot plate at 70 °C for 30 minutes and then in a vacuum oven at 140 °C overnight under vacuum condition to ensure the complete removal of residual moisture. The surface and cross-sectional morphologies were observed on a scanning electron microscope (S-2700, Hitachi, Japan).

2-4. Electrochemical characterization

The electrode was transferred into an argon-filled glove box without being exposed to air. CR2032 coin half-cells were assembled in the glove box with a lithium-metal counter and reference electrode, and a Celgard 2500 separator. 1 M $LiPF_6$ dissolved in a 1:1:1 (v/v/v) mixture of EC (ethylene carbonate)/DMC (dimethyl carbonate)/DEC (diethyl carbonate) was used as the electrolyte. The coin half-cells were galvanostatically discharged to 0.01 V and charged to 1.0 V at a C/10 rate using a cycler (WBCS3000L, WonAtech Co.). Electrochemical impedance spectroscopy (EIS) was performed using an impedance analyzer (ZIVE SP1, WonAtech Co.) after charging at a C/10 rate to 1.00 V or discharging at a C/10 rate to 0.01 V. EIS measurements were carried out using a 30 mV of amplitude in the frequency range of 0.01 Hz to 100 kHz.

3. Results and Discussion

Fig. 2 presents the cyclic performance of PVdF-E, PVA-E and ESPVA-E at a C/10 rate in a voltage window of 0.01~1.0 V. In the 2nd cycle, the discharge capacities of PVdF-E, PVA-E and ESPVA-E reached 485, 796 and 1,083 mAh/g, respectively. The theoretical capacities of Si and graphite (C) are 4,200 and 372 mAh/g [10], so that the capacity of Si/C anode becomes 1,648 mAh/g by proportion. After the 25th cycle, the specific discharge capacity of PVdF-E, PVA-E and ESPVA-E were 132, 64 and 308 mAh/g, respectively. Considering that the 1st cycle contributes to form solid electrolyte interface (SEI) films, the capacity retention ratios at the 25th cycle based on the 2nd cycle were 27%, 8% and 37%, correspondingly.

Especially, PVdF-E showed the worst capacity retention compared to PVA-E and ESPVA-E. *As the charge-discharge* cycle proceeded, cracks must have been formed in the Si/C materials. During the lithiation step of electrochemical alloying, the Si nanoparticles are growing in size, and the binder, which is coated on the particle surface, also undergoes a morphological change induced by the volume expansion of Si particles. During the delithiation step, the lithium is extracted from the alloying and the particles shrink to the initial size. However, the binder is not able to follow the volume change and electrical contacts are lost [19].

As shown in Fig. 2, PVA-E showed better cyclic performance than PVdF-E especially after the 5th cycle due to the higher adhesion strength of PVA. Besides, the hydrogen bonding of hydroxyl groups in PVA

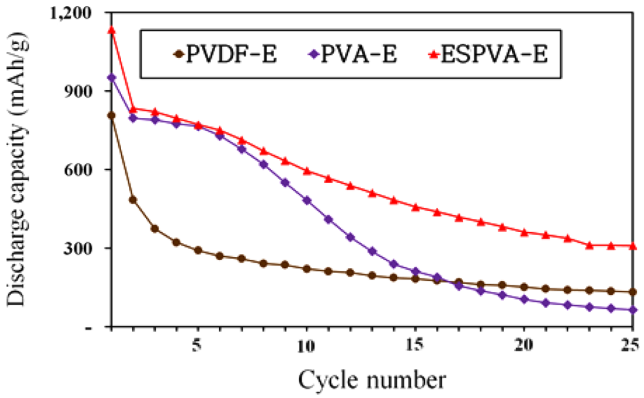

Fig. 2. Cyclic performance of PVdF-E, PVA-E and ESPVA-E.

with Si particles prevented the electrode from cracking. Some researches proposed, on the basis of NMR (nuclear magnetic resonance) studies, that hydroxyl groups in polymeric chains and Si nanoparticles form hydrogen bonding. This hypothesis seems to be the most favorable one, as the hydrogen bonding enables a self-healing process of the electrode upon the volume change [19-21]. However, after the fifth cycle, PVA-E showed a rapid capacity decrease because it might have lost its restoring capacity. This type of curve represents an increase of the resistance of the cell. Meanwhile, the highest capacity retention of ESPVA-E verified its structural stability. Electrospinning process formed PVA nanofibrous matrix in the electrode. Because PVA nanofibers are also elastic, as suggested by the macroscopic property of PVA [22], the mechanical strain during the lithiation is effectively released through the overall PVA nanofibrous structure. Thus, the PVA nanofibrous matrix did not only prevent damages from the volume expansion, but also effectively assigned the self-healing to the electrode during the volume contraction, as confirmed by the comparison of cyclic performance between PVA-E and ESPVA-E in Fig. 2.

Fig. 3 shows the impedance spectra of PVdF-E, PVA-E and ESPVA-E electrodes at the second cycle. In the Nyquist plots of EIS measurements, the left end value means the inductive behavior caused

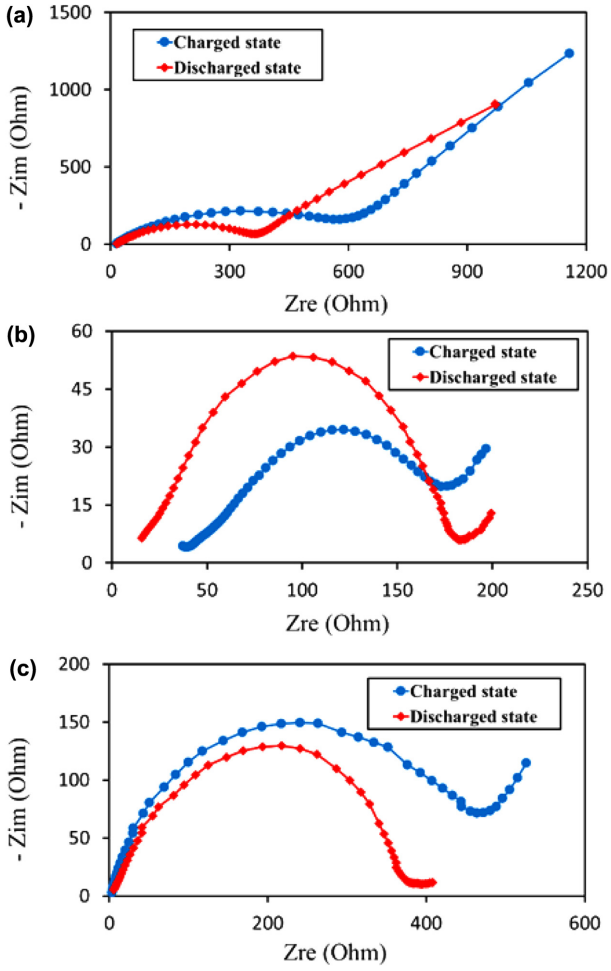

Fig. 3. EIS results of PVDF-E (a), PVA-E (b), and ESPVA-E (c) at the charged and discharged state.

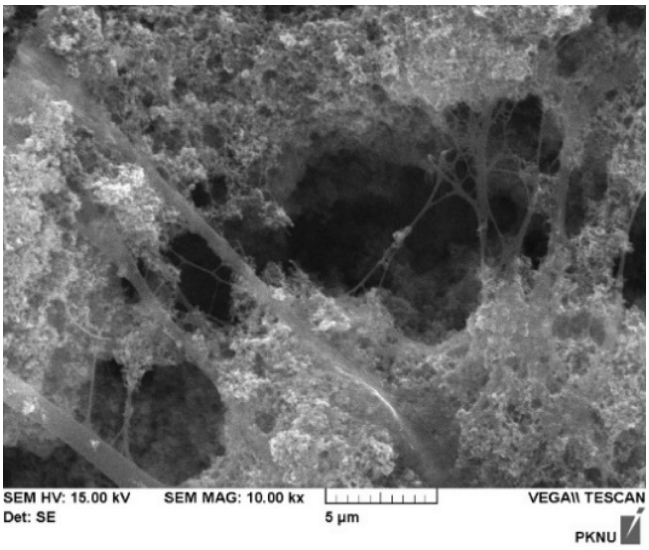

Fig. 4. SEM image of the surface of ESPVA-E.

by inductive reactance of metallic elements in the cell and wire. The semi-circle represents the complex impedance: the SEI and double layer capacity are related to the charge transfer. A high frequency of the semicircle is possibly assigned to the charge transfer resistance, related to the electrochemical reactions between the particles or between the electrode and the electrolyte. The line with an angle of 45° shows diffusion processes in active materials of the electrodes at very low frequencies [23]. First, the charge transfer resistances are generally higher for the charged state than for the discharged state in Fig. 3. It is because of the loss of electrical contact of Si nanoparticles ensuing their contraction by the delithiation at the charged state. Then, the charge transfer resistances of PVdF-E, PVA-E and ESPVA-E electrodes for the charged state (Z_{re} values for the relative maxima of the semi-circles) were 328, 122 and 240 Ω, respectively. The higher resistance of PVdF-E is due to the inferior binding capacity of PVdF compared to PVA; thus, the PVdF binder does not contain the expansion and contraction of Si nanoparticles as well as does the PVA. Then, the higher resistance of ESPVA-E compared to PVA-E is probably attributed to the presence of extra non-conducting constituents, that is, electrospun PVA nanofibers. It might assign electrical conductivity to nanofibers by using conducting polymers [24,25] or carbonization [26], metallic doping [27], and modification [28] of electrospun nanofibers.

The PVA nanofibrous structure fabricated by electrospinning is also confirmed through the SEM images shown in Fig. 4. The PVA nanofiber has a thickness of < 1 mm. Good elasticity of PVA nanofibers is expected to let the mechanical stress to be released throughout the overall structure.

4. Conclusions

Si/C anodes with electrospun PVA nanofibers exhibited enhanced cycling stability (55% capacity retention ratio) compared to electrodes with PVdF and PVA binders (38% and 23%, respectively). The result

probably comes from the combined effect of the hydrogen bonding of PVA binder and structural stability of the electrospun PVA nanofibrous matrix. Further studies are required to decrease the impedance by introducing some conductivity to the electrospun nanofibers.

Acknowledgments

This work was supported by the Pukyong National University Research Abroad Fund in 2016 (C-D-2016-0848).

References

1. Scrosati, B. and Garche, J., "Lithium Batteries: Status, Prospects and Future," *J. Power Sources*, **195**, 2419-2430(2010).
2. Namiki, F., Maeshima, T., Inoue, K., Kawai, H., Saibara, S. and Nanto, T., "Lithium-ion Battery for HEVs, PHEVs, and EVs," *Hitachi Review*, **63**, 103-108(2014).
3. Tarascon, J. -M. and Armand, M., "Issues and Challenges Facing Rechargeable Lithium Batteries," *Nature*, **414**, 359-367(2001).
4. Huggins, R. A., "Lithium Alloy Negative Electrodes," *J. Power Sources*, **81**, 13-19(1999).
5. Chan, C. K., Zhang, X. F. and Cui, Y., "High Capacity Li Ion Battery Anodes Using Ge Nanowires," *Nano Lett.*, **8**, 307-309 (2008).
6. Zhang, W. J., "A Review of the Electrochemical Performance of Alloy Anodes for Lithium-ion Batteries," *J. Power Sources*, **196**, 13-24(2011).
7. Szczech, J. R. and Jin, S., "Nanostructured Silicon for High Capacity Lithium Battery Anodes," *Energy & Environ. Sci*., **4**, 56-72 (2011).
8. Kasavajjula, U., Wang, C. S. and Appleby, A. J., "Nano-and Bulk-silicon-based Insertion Anodes for Lithium-ion Secondary Cells," *J. Power Sources*, **163**, 1003-1039(2007).
9. Beaulieu, L. Y., Eberman, K. W., Turner, R. L., Krause, L. J. and Dahn, J. R., "Colossal Reversible Volume Changes in Lithium Alloys," *Electrochem. Solid-State Lett*., **4**, A137-A140(2001).
10. Beaulieu, L. Y., Hatchard, T. D., Bonakdarpour, A., Fleischauer, M. D. and Dahn, J. R., "Reaction of Li with Alloy Thin Films Studied by In Situ AFM," *J. Electrochem. Soc*., **150**, A1457-A1464(2003).
11. Hertzberg, B., Alexeev, A. and Yushin, G., "Deformations in Si-Li Anodes Upon Electrochemical Alloying in Nano-Confined Space," *J. Am. Chem. Soc*., **132**, 8548-8549(2010).
12. Graetz, J., Ahn, C. C., Yazami, R. and Fultz, B., "Highly Reversible Lithium Storage in Nanostructured Silicon," *Electrochem. Solid-State Lett*., **6**, A194-A197(2003).
13. Liu, X. H., Huang, L. S., Mao, S. X., Zhu, T. and Huang, J. Y., "Size-Dependent Fracture of Silicon Nanoparticles during Lithiation," *ACS Nano*., **6**, 1522-1531(2012).
14. Liu, X. H., Zheng, H., Zhong, L., Huang, S., Karki, K., Zhang, L. Q. and Cho, J. H., "Anisotropic Swelling and Fracture of Silicon Nanowires During Lithiation," *Nano Lett*., **11**, 3312-3318(2011).
15. Lee, S. W., Lee, H. W., Nix, W. D., Gao, H. and Cui, Y., "Kinetics and Fracture Resistance of Lithiated Silicon Nanostructure Pairs Controlled by Their Mechanical Interaction," *Nature Comm*., **6** (2015).
16. Chen, J., Liu, J., Qi, Y., Sun, T. and Li, X., "Unveiling the Roles of Binder in the Mechanical Integrity of Electrodes for Lithium-Ion Batteries," *J. Electrochem. Soc.*, **160**, A1502-A1509(2013).
17. Chen, Z., Christensen, L. and Dahn, J. R., "Comparison of PVDF and PVDF-TFE-P as Binders for Electrode Materials Showing Large Volume Changes in Lithium-Ion Batteries," *J. Electrochem. Soc.,* **150**, A1073-A1078(2003).
18. Chen, Z., Christensen, L. and Dahn, J. R., "A Study of the Mechanical and Electrical Properties of a Polymer/carbon Black Binder System Used in Battery Electrodes," *J. Appl. Polym. Sci.,* **90**, 1891-1899(2003).
19. Munao, D., Van Erven, J. W. M., Valvo, M., Garcia-Tamayo, E. and Kelder, E. M. "Role of the Binder on the Failure Mechanism of Si Nano-composite Electrodes for Li-ion Batteries," *J. Power Sources*., **196**, 6695-6702(2011).
20. Park, H. K., Kong, B. S. and Oh, E. S., "Effect of High Adhesive Polyvinyl Alcohol Binder on the Anodes of Lithium Ion Batteries," *Electrochem. Comm*., **13**, 1051-1053(2011).
21. Bridel, J. S., Azais, T., Morcrette, M., Tarascon, J. M. and Larcher, D., "Key Parameters Governing the Reversibility of Si/Carbon/CMC Electrodes for Li-Ion Batteries," *Chem. Mater*., **22**, 1229-1241(2009).
22. Janković, B., Pelipenko, J., Škarabot, M., Muševič, I. and Kristl, J., "The Design Trend in Tissue-engineering Scaffolds based on Nanomechanical Properties of Individual Electrospun Nanofibers," *Inter. J. pharm.,* **455**, 338-347(2013).
23. Andre, D., Meiler, M., Steiner, K., Wimmer, C., Soczka-Guth, T. and Sauer, D. U., "Characterization of High-power Lithium-ion Batteries by Electrochemical Impedance Spectroscopy. I. Experimental Investigation," *J. Power Sources*., **196**, 5334-5341(2011).
24. Prabhakaran, M. P., Ghasemi-Mobarakeh, L., Jin, G. and Ramakrishna, S., "Electrospun Conducting Polymer Nanofibers and Electrical Stimulation of Nerve Stem Cells," *J. Biosci. Bioeng*., **112**, 501-507(2011).
25. Zhang, Y. and Rutledge, G. C., "Electrical Conductivity of Electrospun Polyaniline and Polyaniline-Blend Fibers and Mats," *Macromolecules*, **45**, 4238-4246(2012).
26. Panapoy, M., Dankeaw, A. and Ksapabutr, B., "Electrical Conductivity of PAN-based Carbon Nanofibers Prepared by Electrospinning Method," *Thammasat Int. J. Sc. Tech*., **13**, 11-17(2008).
27. Wang, W., Li, Z., Xu, X., Dong, B., Zhang, H., Wang, Z. and Fang, S., "Au-Doped Polyacrylonitrile–Polyaniline Core–Shell Electrospun Nanofibers Having High Field-Effect Mobilities," *Small*, **7**, 597-600(2011).
28. Heikkilä, P. and Harlin, A., "Electrospinning of Polyacrylonitrile (PAN) Solution: Effect of Conductive Additive and Filler on the Process," *Express Polym. Lett.,* **3**, 437-445(2009).